

Nature of the broadband luminescence center in MgO:Cr³⁺

M. O. Henry, J. P. Larkin, and G. F. Imbusch
Department of Physics, University College, Galway, Ireland
 (Received 22 September 1975)

The luminescence spectrum of MgO:Cr³⁺ is characterized by a series of sharp features at around 7000 Å and a broad band which stretches from about 7000 Å to 1 μm. The nature of the centers responsible for this broadband luminescence is examined by a combination of phase-sensitive detection methods and polarized absorption and luminescence methods. The phase-sensitive detection method allows us to separate clearly the broadband luminescence from the remainder of the spectrum and a sharp no-phonon line associated with the broadband luminescence is uncovered. The centers responsible for the broadband luminescence are found to have axes of symmetry along [011]-type directions, supporting the conclusion that this luminescence originates on Cr³⁺ ions in rhombic centers. At high temperatures broad emission is also observed from cubic site Cr³⁺ ions. The cubic site luminescence is shown to behave in accordance with theoretical expectations.

I. INTRODUCTION

The luminescence spectrum of MgO:Cr³⁺ is characterized by sharp features at around 7000 Å and a broad apparently featureless band stretching from around 7000 Å to 1 μm. In this work we describe experimental measurements to determine the nature of the centers which are responsible for this broadband luminescence.

In MgO:Cr³⁺ the chromium ions enter substitutionally for magnesium ions. When a Cr³⁺ ion substitutes for a Mg²⁺ ion a charge imbalance is created and to compensate for this imbalance vacancies occur in some Mg²⁺ sites. EPR studies¹⁻³ have shown that a large fraction of the Cr³⁺ ions do not have charge compensating vacancies nearby and so are in sites of perfect octahedral symmetry (cubic sites). Of the Cr³⁺ ions in the vicinity of a vacancy most have the vacancy along [001]-type directions, and this lowers the symmetry of the Cr³⁺ site from cubic to tetragonal. A smaller number have the vacancy along the [011]-type direction, and this lowers the site symmetry to rhombic. The presence of these nearby vacancies changes the crystal field at the Cr³⁺ site causing a shift and splitting of the Cr³⁺ energy levels.^{4,5}

It has been shown that the chromium ions in cubic and tetragonal sites are responsible for the strong sharp features at around 7000 Å.^{4,5} The chromium ions in rhombic sites, although they occur in reasonable abundance, do not contribute to the strong sharp-line features near 7000 Å. In a recent publication⁶ Castelli and Forster showed that the broadband luminescence from MgO:Cr³⁺ does not originate on the centers responsible for the strong sharp features around 7000 Å. They attribute the broadband to luminescence from Cr³⁺ ions in rhombic sites. In this study we show that the centers responsible for the broadband luminescence at low temperatures have [011]-type symmetry. This affords strong support to

Castelli and Forster's assertion that Cr³⁺ ions in rhombic sites are responsible for the broadband luminescence.

By using phase-sensitive detection methods we have separated the rhombic-site luminescence from the rest of the spectrum and we find that it contains some structure including what appears to be a ⁴T₂ - ⁴A₂ no-phonon transition at 7315 Å, about 1690 cm⁻¹ lower than the corresponding transition on the Cr³⁺ ion in a cubic site. This shift in energy is to be expected since the ⁴T₂ - ⁴A₂ separation is very sensitive to changes in the crystal field.⁷ On the other hand, the ²E - ⁴A₂ separation is much less sensitive to changes in crystal field so that the position of the ²E - ⁴A₂ no-phonon transition should be close to the corresponding transitions on Cr³⁺ ions in cubic and tetragonal sites, that is, it should be close to 7000 Å. Consequently the ⁴T₂ level would appear to lie below the ²E level for the rhombic-site ion, and luminescence should be found only from the ⁴T₂ level of this ion.

At high temperatures an additional broadband luminescence due to ⁴T₂ - ⁴A₂ emission from cubic-site ions occurs. This cubic-site luminescence can be separated from the rhombic-site luminescence by phase-sensitive detection methods and the temperature dependence of the shape and lifetime of this cubic-site luminescence shows good agreement with theoretical estimates.

In Sec. II we review the general spectroscopic features of MgO:Cr³⁺. We then describe the experimental methods employed by us. The experimental results are discussed and from these we draw a fairly comprehensive picture of the various luminescence centers in MgO:Cr³⁺.

II. LUMINESCENCE SPECTRUM OF MgO:Cr³⁺

The luminescence spectrum under continuous optical pumping of a lightly doped MgO:Cr³⁺ crystal at 77 K is shown in Fig. 1(a). This shows the

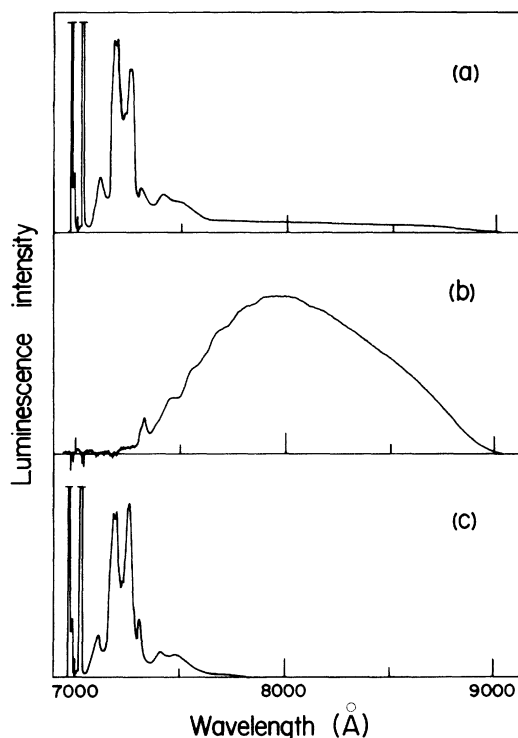


FIG. 1. Luminescence spectrum of $\text{MgO}:\text{Cr}^{3+}$ at 77 K: (a) under unmodulated optical pumping; (b) phase-sensitive detector output where the phase is set to null the slowly decaying component; (c) phase-sensitive detector output when the phase is set to null the fast decaying component. A photomultiplier tube whose response drops to zero at around 9000 Å was used.

strong sharp lines near 7000 Å as well as the broadband which stretches from around 7000 Å to 1 μ . Because of its high quantum efficiency, an RCA C31034 photomultiplier tube was used in obtaining this trace. Since this detector is not sensitive beyond 9000 Å, the broadband appears to drop to zero at this wavelength. The R line at 6981 Å is the no-phonon ${}^2E \rightarrow {}^4A_2$ line from Cr^{3+} ions in cubic sites.⁴ The N_2 line at 7038 Å as well as the line at 6992 Å are no-phonon ${}^2E \rightarrow {}^4A_2$ lines from the split 2E level of Cr^{3+} ions in Cr-vacancy centers where the vacancy is in the nearest-cation-neighbor site along [001]-type directions⁵ (tetragonal sites). Such centers were first seen in EPR measurements.¹ The N_1 line at 7035 Å and the line at 6989 Å are believed to be no-phonon ${}^2E \rightarrow {}^4A_2$ lines from Cr-vacancy-Cr centers, where the Cr^{3+} ions are on either side of a [001]-type vacancy.⁵ These Cr-vacancy and Cr-vacancy-Cr centers are illustrated in Fig. 2. Rhombic-site Cr^{3+} ions with a vacancy in the nearest-cation-neighbor site along a [011]-type direction occur in this material (Fig. 2) and were first seen in EPR measurements,² but they do not contribute to the strong sharp features around 7000 Å.⁸

Weak sharp lines at 7082 and 7086 Å which have been attributed to rhombic sites⁹ will be discussed later. Larkin *et al.*⁸ pointed out that the perturbed crystal field at this rhombic site could cause the 4T_2 level of the Cr^{3+} ion to be below 2E so that luminescence would occur only from the 4T_2 level of such ions and as a result no strong sharp ${}^2E \rightarrow {}^4A_2$ transitions from rhombic sites would be found. Cr^{3+} ions with a vacancy in a nearby cation site along a [111]-type direction have never been reported in EPR experiments. In such a center there would be at least one oxygen ion between the Cr^{3+} ion and the vacancy, and the Cr-vacancy separation would be greater by a factor of $\sqrt{3}$; 1 than in the tetragonal site, and consequently the Cr^{3+} ion should be perturbed by the vacancy to a smaller extent than the Cr^{3+} ion in the tetragonal site. Such centers might be expected to show sharp ${}^2E \rightarrow {}^4A_2$ lines between the R and N lines. No such lines are seen and so the optical evidence supports the EPR evidence that such [111]-type centers do not occur. We shall not consider them further.

The vibrational sidebands of the R and N lines have been examined by a number of workers.^{6,10,11} The band at 7110 Å is the acoustical sideband of the R line while the optical sideband of the R line has a major peak at around 7180 Å and a weaker peak at 7410 Å. The acoustical sideband of the N lines peaks at 7190 Å where it coincides with the optical sideband of the R line. The optical sideband of the N lines has major and minor peaks at 7250 and 7490 Å, respectively.

The lifetime at 77 K of the R and N lines are similar but clearly different from each other, being 11.6 and 8.6 msec, respectively, in our sample. The lifetime of the sideband luminescence is, of course, identical with that of the no-phonon

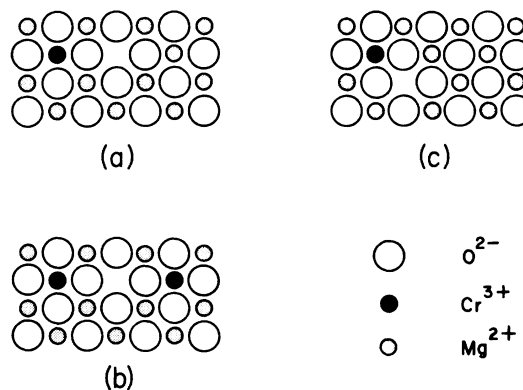


FIG. 2. Representation of the yz plane of MgO showing the environments of Cr^{3+} ions in noncubic sites: (a) tetragonal Cr-vacancy center, [001] symmetry; (b) tetragonal Cr-vacancy-Cr center, [001] symmetry; (c) rhombic Cr-vacancy center, [011] symmetry.

line associated with it. These lifetimes vary with temperature, dropping to about 1 msec at room temperature. In contrast with this millisecond lifetime the broadband luminescence which stretches from 7000 Å to 1 μ and which peaks at around 8000 Å has a lifetime of 35 μsec.⁶

Parker *et al.*¹² first drew attention to this broadband luminescence and quite correctly pointed out that with its position and lifetime it has the characteristics of ${}^4T_2 - {}^4A_2$ emission from Cr^{3+} ions. They attributed it to Cr^{3+} ions in cubic sites. But it is difficult to visualize luminescence occurring from both the 4T_2 and the 2E levels of the same center at low temperature and with distinct lifetimes, since the ${}^4T_2 - {}^2E$ nonradiative relaxation rate is typically around 10^{11} sec^{-1} .¹³ Castelli and Forster⁶ showed that the broadband luminescence does not come from cubic or tetragonal site Cr ions since the absorption bands of the centers responsible for the broadband luminescence are quite different from the absorption bands of the cubic and tetragonal sites. Consequently they assigned the broadband luminescence to Cr^{3+} ions in rhombic sites. Our own excitation experiments had indicated that the centers for the broadband and sharp-line luminescence were distinct and we set ourselves the task of trying to establish experimentally the nature of the broadband luminescence center.

III. EXPERIMENTAL METHODS

A. Excitation spectra

High-resolution excitation spectra of the R and N lines, of their sidebands, and of the broadband luminescence were taken at 77 K. The output of a Sylvania DVY 650-W tungsten iodide lamp was passed through a $\frac{1}{4}$ -m monochromator and focussed onto the sample, which was immersed in a Dewar of liquid nitrogen. The luminescence from the sample was passed through another $\frac{1}{4}$ -m monochromator, detected by an RCA C31034 photomultiplier tube and displayed on a chart recorder. The second monochromator could be adjusted to select the R line, the N lines, their vibrational sidebands or the broadband, so that by scanning with the first monochromator, the individual excitation spectra could be taken. Some of these are shown in Fig. 3. The spectra are not corrected for variations with wavelength in the response of the system. When these corrections are made, the bands at shorter wavelengths are stronger in each of the three spectra shown.

B. Phase-sensitive detection of luminescence

The technique of phase-sensitive detection is widely used in signal recovery. For luminescence studies one modulates the exciting light at some

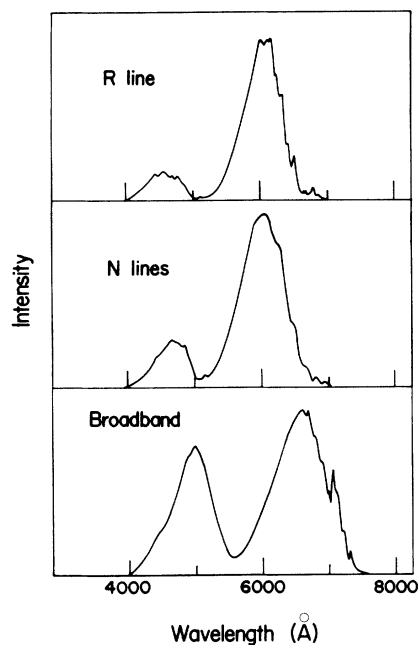


FIG. 3. Excitation spectra of the R line, N lines, and broadband luminescence at 77 K. These have not been corrected for the spectral characteristics of the exciting light and monochromator.

frequency ω_m and looks for a component of this frequency in the luminescence signal V_s . This can be done as follows. A reference voltage V_r at frequency ω_m obtained from the modulator switches the output signal V_s on and off every half cycle. When the reference and signal are of the same frequency and phase, the phase-sensitive detector acts as a rectifier and gives an average dc voltage V_0 proportional to the amplitude of the signal V_s . When they are in antiphase, the dc output is reversed. When the signal and reference are in quadrature, the average output is zero, and we can say that the signal has been "phased out" or "nulled."

Because of phase changes within the electronics, and especially because of the finite relaxation time of the luminescence, the output signal V_s is in general not in phase with the reference signal. To maximize the dc output voltage V_0 the phase of the reference voltage V_r is adjusted to be in phase with the signal V_s . If the luminescence signal consists of two components with different relaxation times, then V_{s1} and V_{s2} , the modulated components of these two signals, will be out of phase with each other. If one adjusts the phase of the reference to maximize V_{s1} , say, then the strength of the other will appear weaker. Furthermore, if one adjusts the phase of the reference to null one component, the other component will not be nulled and will give an output signal.

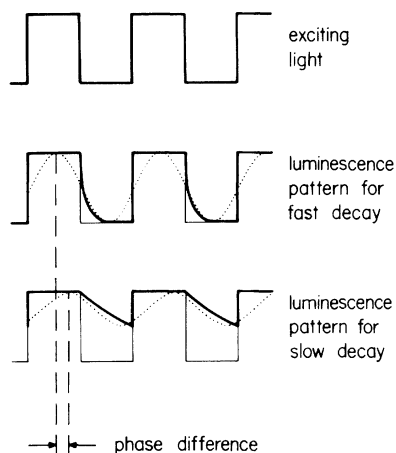


FIG. 4. Responses of the fast and slowly decaying luminescence signals under square-wave optical excitation are different. In particular, the main sinusoidal components at the modulating frequency are out of phase with each other. A phase-sensitive detector which detects only the main Fourier component of the luminescence signal will have different phase settings for the fast and slow components. When the phase of the detector is set to null one component the other will still give a signal. In this way the spectra from two luminescence centers with different decay times can be separated from each other.

The way in which the phase differences occur in the output is shown in Fig. 4. This affords us a method of separating two luminescence signals which overlap in wavelength—and which have different relaxation times. This method has been used to great advantage by Engstrom and Molle-
nauer to separate the luminescence spectra of various Cr-pair centers in ruby.¹⁴

Because of the very different lifetimes of, on the one hand, the *R* and *N* lines and their sidebands (~ 10 msec), and on the other hand, the broadband luminescence (~ 35 μ sec), it was a relatively simple matter to null the broadband and look only at the sharp-line spectrum [Fig. 1(c)]. Nulling the sharp lines and looking only at the broadband [Fig. 1(b)] was a little more difficult since the *R* and *N* line lifetimes are not exactly the same—they are 11.6 and 8.6 msec, respectively, at 77 K in our sample—and some faint residual lines are seen. These do not complicate matters, but rather serve as useful wavelength markers. Figure 1(b) shows that the broadband luminescence has some fine structure on its short-wavelength side which was completely masked by the stronger sharp features of the sidebands of the *R* and *N* lines. The slight difference in the lifetimes of the *R* and *N* lines distorts the relative amplitudes of the phase-sensitive detector output for these two lines and for their sidebands. This can be seen by comparing the sideband amplitudes

in Figs. 1(a) and 1(c). In these experiments the exciting light was chopped with a Brookdeal light chopper (model 9479) and the signal recovered through a Brookdeal phase-sensitive detector (model 9501) which, with its very fine control of phase, is ideal for this type of work.

At high temperatures the lifetimes of the two components of the luminescence are still quite distinct and the above method of separation can still be employed.

C. Polarized absorption and luminescence

Luminescence from individual centers in sites of cubic symmetry is completely unpolarized, but ions in sites of axial symmetry will individually be expected to exhibit anisotropy. When the axes of all the centers in a crystal point along the same direction the absorption and luminescence of the crystal will exhibit this anisotropy (e.g., $\text{Al}_2\text{O}_3:\text{Cr}^{3+}$). In a cubic crystal, however, such as $\text{MgO}:\text{Cr}^{3+}$, with such axial centers equally distributed among all possible orientations, the over-all absorption is isotropic. If such a crystal is excited with unpolarized light so that the ions in the uniaxial sites are raised to excited states, the resultant luminescence from the crystal is isotropic, even though the individual centers emit anisotropically. By exciting with light polarized along one of the site axes, those centers whose axes are in this direction will absorb to a different degree than the other centers and consequently the luminescence from the sample will be anisotropic. This method has been widely used in the study of color centers in alkali halides¹⁵⁻¹⁷ and was first used by Feofilov¹⁸ to determine the symmetry of luminescence centers in cubic crystals. We used this method to determine whether or not the centers giving rise to the broadband luminescence have [011]-type symmetry. We illustrate the method quantitatively with the aid of Fig. 5.

The crystal was mounted so that its (100) face was normal to the direction of the exciting light, and the luminescence in the $[\bar{1}00]$ direction was recorded using a phase-sensitive detector adjusted so that only the broadband emission was recovered. Type HN22 polaroids were used to polarize both the exciting light and the luminescence from the crystal. The intensity of the broadband luminescence polarized with its electric vector along [011] was measured for different polarizations of the exciting light, and the results are shown in Fig. 6.

Consider the case where we are dealing with ions in uniaxial centers where in each case the axis of symmetry is along a [011]-type direction ([011]-type centers). In $\text{MgO}:\text{Cr}^{3+}$ there are six inequivalent [011]-type centers, as shown in Fig. 5, and we assume that the numbers of chromium ions in all such centers are the same. If A_b and A_v

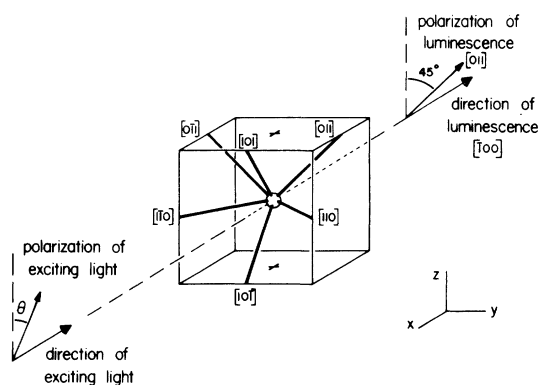


FIG. 5. Experimental configuration for the polarized absorption/luminescence measurements. The six inequivalent [011]-type centers are shown schematically, as well as the directions and polarizations of the exciting light and of the luminescence. Optical filters in front of the spectrometer slit prevented the exciting light from reaching the detector.

are, respectively, the absorption strengths for the absorption of light polarized parallel and perpendicular to the axis of the center, then the absorption strength (and hence the optical pumping efficiency of this center) for light polarized at an angle ϕ to the axis goes as $A_p \cos^2 \phi + A_v \sin^2 \phi$. By applying this formula to each of the six centers we can estimate the relative excited state populations of the centers as a function of the polarization of the exciting light. We now assume that the luminescence output of the centers is anisotropic, the emission strengths being E_p and E_v for emission polarized parallel and perpendicular to the axis, respectively. In this way we can obtain an expression for the relative intensity of the luminescence being emitted in the $[100]$ direction and polarized along the $[011]$ direction as a function of the polarization angle θ of the exciting light. The intensity of the exciting light is maintained at a constant value irrespective of the polarization angle θ . The expression for the luminescence intensity as a function of θ is

$$I(\theta) = \frac{1}{4}(E_p + 3E_v)(A_p + 3A_v) + \frac{1}{2}(E_p + E_v)(A_p + A_v) + \frac{1}{2}(E_p - E_v)(A_p - A_v) \sin 2\theta \quad (1)$$

This angular pattern is seen to have turning points for polarization angles $\theta = 45^\circ$ and 135° , which correspond to the exciting light being polarized along the $[011]$ and $[0\bar{1}1]$ directions, respectively.

It is of interest to consider the corresponding emission from ions in uniaxial centers with symmetry axes along $[001]$ -type directions ($[001]$ -type centers). There are three inequivalent $[001]$ -type centers in $\text{MgO}:\text{Cr}^{3+}$. A mathematical treatment similar to that carried out above for the $[011]$ -type centers shows that the intensity of the lumines-

cence emitted from $[001]$ -type centers in the $[\bar{1}00]$ direction and polarized along $[011]$ is independent of the polarization angle θ of the exciting light. This difference between the angular patterns of the luminescence intensity from the $[011]$ - and $[001]$ -type centers can be used to establish whether or not $[011]$ -type centers contribute to the broadband luminescence from $\text{MgO}:\text{Cr}^{3+}$.

IV. EXPERIMENTAL RESULTS

A normal luminescence spectrum of a lightly doped $\text{MgO}:\text{Cr}^{3+}$ sample obtained under unmodulated optical pumping is shown in Fig. 1(a). The spectrum is not corrected for variations with wavelength in the response of the system, but the response is fairly flat over the range 7000–8500 Å. Figures 1(b) and 1(c) show luminescence spectra taken with the phase-sensitive detector. For Fig. 1(b) the luminescence from cubic and tetragonal site ions is nulled, so that the broadband only is recovered. The high-energy side of this band shows a succession of features dominated by a sharp line at 7315 Å. For Fig. 1(c) the broadband luminescence is nulled, so that luminescence from cubic and tetragonal sites only is recovered. This shows the extent of the *R* line and *N* lines sidebands at 77 K. It is seen that at these tempera-

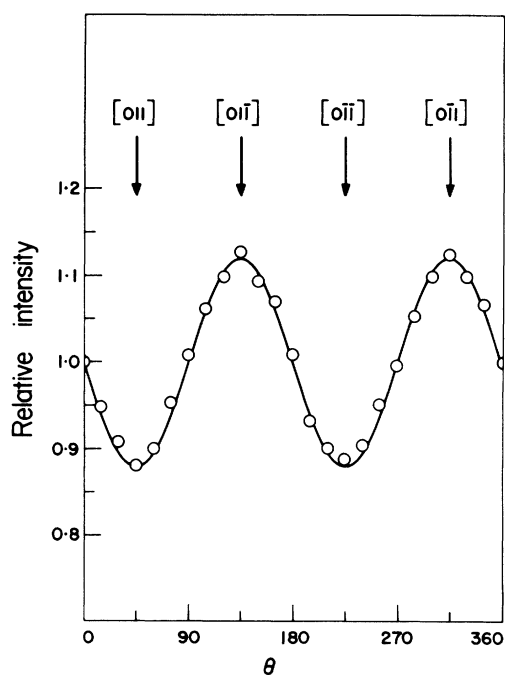


FIG. 6. Measured values (open circles) of the intensity of the broadband luminescence emitted in the $[100]$ direction and polarized along the $[011]$ direction as a function of the polarization angle θ of the exciting light. Arrows indicate the values of θ for which extrema are predicted for luminescence from $[011]$ -type centers.

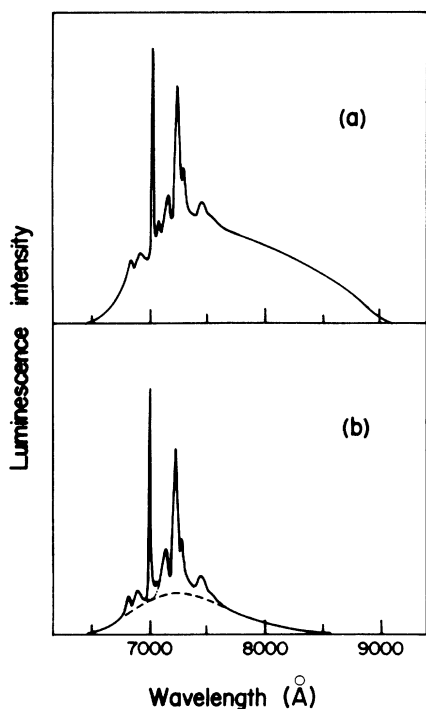


FIG. 7. Room-temperature luminescence spectra of $\text{MgO}:\text{Cr}^{3+}$: (a) under unmodulated optical pumping; (b) phase-sensitive detector output where the phase is set to null the fast decaying component.

tures no broadband luminescence is emitted by the cubic or tetragonal site ions. Because of the difference in their lifetimes, the R line and N lines luminescence could also be separated by using phase-sensitive detection methods, but in these cases some broadband luminescence is also recovered. However, we could get a measure of the intensity ratio of sidebands to no-phonon line for both the R line and the N lines (unresolved). For cubic sites we found an intensity ratio of 4:1 while for the tetragonal sites the ratio is 4.8:1 in our sample. The first of these values is smaller than that reported by Castelli and Forster.⁶

A normal luminescence spectrum obtained under unmodulated optical pumping at room temperature is shown in Fig. 7(a). The intensity of the N lines emission has dropped significantly relative to that of the R line compared to the 77-K spectrum [Fig. 1(a)]. Anti-Stokes sidebands are seen on the high-energy side of the no-phonon lines, and the broadband luminescence stretches down to shorter wavelengths. Figure 7(b) shows a phase-sensitive spectrum at room temperature for which the broadband luminescence is nulled. This spectrum shows that at higher temperatures some broadband luminescence is emitted by cubic and, to a lesser degree, tetragonal site ions, and it stretches to about 8500 Å. At temperatures above 300 K the N lines

are no longer seen in the luminescence spectrum. The dotted curve in Fig. 7(b) indicates the separation between the no-phonon lines and the rest of the spectrum.

Excitation spectra of the R line, N lines, and broadband luminescence at 77 K are shown in Fig. 3. Excitation spectra of the R , N_1 , and N_2 lines have been previously examined by Fairbank and Klauminzer,¹⁹ and Castelli and Forster⁶ have recorded the broadband excitation spectrum. Each of the spectra in Fig. 3 consists of two broad bands with additional structure. The band at shorter wavelengths corresponds to absorption into the 4T_1 level, while that at longer wavelengths corresponds to absorption into the 4T_2 level of Cr^{3+} ions in the various sites. The R line excitation spectrum shows a number of features on the high-energy side of the 4T_2 band. The sharpest feature at 6508 Å is assigned by us to the ${}^4A_2 - {}^4T_2$ no-phonon transition. The excitation spectra show that the 4T_1 and 4T_2 levels for tetragonal site ions are at approximately the same positions as those for cubic site ions, but for the tetragonal sites there is no dominant feature which can be identified with the ${}^4A_2 - {}^4T_2$ transition. The broadband excitation spectrum shows that for the Cr^{3+} ions giving rise to this luminescence, the 4T_1 and 4T_2 levels are moved to much lower energies, as Castelli and Forster⁶ first pointed out. The high-energy side of the 4T_2 band of the broadband excitation spectrum shows quite an amount of structure. The main features are a fairly broad line at around 7040 Å, and another sharper line at 7315 Å, which coincides with the sharp line in the broadband luminescence spectrum [Fig. 1(b)].

To determine the symmetry of the center giving rise to the broadband luminescence, we carried out the polarized absorption and luminescence experiment described previously. The intensity of the luminescence being emitted in the $[\bar{1}00]$ direction and polarized along the $[011]$ direction was measured as a function of the polarization angle θ of the exciting light (Fig. 5). We study the luminescence pattern to determine whether or not $[011]$ -type centers contribute to the broadband luminescence.

V. ORIGIN OF BROADBAND LUMINESCENCE

We have already discussed, with the aid of Fig. 5, the dependence of the luminescence intensity from $[011]$ -type centers on the polarization angle of the exciting light. This dependence is given by Eq. (1), which predicts an angular pattern with extrema where θ is 45° , 135° , 225° , and 315° . The experimentally observed behavior of the broadband luminescence is shown in Fig. 6 and shows just such extrema. Luminescence from $[001]$ -type centers, on the other hand, should have no depen-

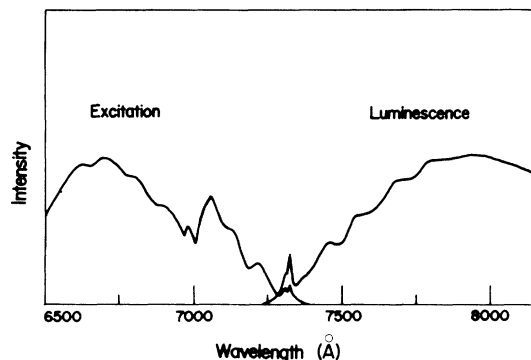


FIG. 8. Details of the excitation and luminescence spectra of the [011]-type Cr^{3+} centers at 77 K.

dence on θ . Consequently, we can say that at least some of the broadband luminescence is due to Cr^{3+} ions in [011]-type sites.

An immediate candidate for the Cr^{3+} ion in a [011]-type site is the rhombic-site ion, represented in Fig. 2, which is known from clear EPR evidence to exist in good quantity, and which does not contribute to the strong sharp luminescence around 7000 Å. We conclude that these rhombic-site Cr^{3+} ions are responsible for at least some of the broadband luminescence. Our data do not preclude the possibility that [001]-type Cr^{3+} centers or cubic Cr^{3+} centers could be partly responsible for the broadband luminescence. Recently, pairs of Cr^{3+} ions in nearest-neighbor cation sites along [001]-type directions have been reported in EPR experiments,²⁰ and such Cr^{3+} centers might emit broad luminescence. We found, however, no evidence to suggest that the broadband luminescence consists of two or more overlapping bands, and we are inclined to attribute the broadband luminescence completely to the rhombic-site Cr^{3+} ions—as Castelli and Forster suggest.⁶

This point of view is consistent with the model of the rhombic center (Fig. 2). The close proximity of the vacancy introduces a large perturbation and should cause a strong shift in the energy levels. The absence of a Mg^{2+} ion should lead to a large reduction in the cubic component of the crystal field, and this should lead to a lowering of the position of the 4T_2 level relative to the ground state. The effect on the energy of the 2E state is expected to be much less pronounced. It is reasonable, then, to expect that the 4T_2 level of the rhombic site ion should lie below the 2E , and so the luminescence from this center should consist of a broad ${}^4T_2 \rightarrow {}^4A_2$ band, Stokes shifted by about 2500 cm^{-1} from the ${}^4A_2 \rightarrow {}^4T_2$ absorption band in the same center (measured in excitation), with, perhaps, a no-phonon line common to both bands at the low-wavelength side of the luminescence band, and with a decay time of 10–50 μsec . These

are precisely the features of the broadband luminescence seen in $\text{MgO}:\text{Cr}^{3+}$ (Fig. 8).

VI. SOME ENERGY LEVELS OF RHOMBIC-SITE Cr^{3+} IONS

Figure 8 shows parts of the broadband excitation (${}^4A_2 \rightarrow {}^4T_2$) and luminescence (${}^4T_2 \rightarrow {}^4A_2$) spectra, and a common feature is the line at 7315 Å. We interpret this line as the ${}^4A_2 \rightarrow {}^4T_2$ no-phonon transition. Closer examination of this line in luminescence shows that it is a doublet of about 30-cm^{-1} separation. Since we do not expect that the position of the 2E level of the rhombic-site Cr^{3+} ion will be much different from its position in the cubic and tetragonal sites, the extra absorption feature seen at 7040 Å in the excitation trace may be the ${}^4A_2 \rightarrow {}^2E$ transition on the rhombic-site ion. Absorption at around this wavelength was previously observed in $\text{MgO}:\text{Cr}^{3+}$ crystals.⁸

Some weak sharp lines, seen in luminescence at 7082 and 7086 Å, have been attributed to transitions on rhombic-site Cr^{3+} ions.⁹ Polarized absorption and luminescence measurements similar to those made for the broadband luminescence show that these lines do originate on either [011]- or [111]-type centers. However, we do not believe⁸ that these are the no-phonon ${}^2E \rightarrow {}^4A_2$ transition on the rhombic center. Some other very faint lines are seen in the luminescence spectrum of $\text{MgO}:\text{Cr}^{3+}$, and we are examining the symmetry of the centers which give rise to these lines by the polarized absorption and luminescence method.

VII. TEMPERATURE DEPENDENCE OF CUBIC-SITE LUMINESCENCE

At 77 K luminescence is observed from cubic sites (R line plus sidebands), from tetragonal sites (N lines plus sidebands), and from rhombic sites (broadband). These are seen in Fig. 1(a). At room temperature [Fig. 7(a)] the no-phonon lines have broadened, and the relative intensity of the tetragonal-site luminescence has dropped significantly. Above 300 K luminescence from these sites seems to disappear completely and we are left with only cubic- and rhombic-site luminescence. By using phase-sensitive detection methods we have been able to null the rhombic luminescence, and we have studied the remaining cubic-site luminescence as a function of temperature.

Figure 7(b) shows such a room-temperature spectrum containing a small residual amount of N line luminescence which we neglect in the analysis. The anti-Stokes sidebands show up on the high-energy side of the R line, and both the R line and sidebands appear to be superimposed upon a broadband stretching from around 6500 to 8500 Å. At higher temperatures we expect a broadband luminescence to occur from the 4T_2

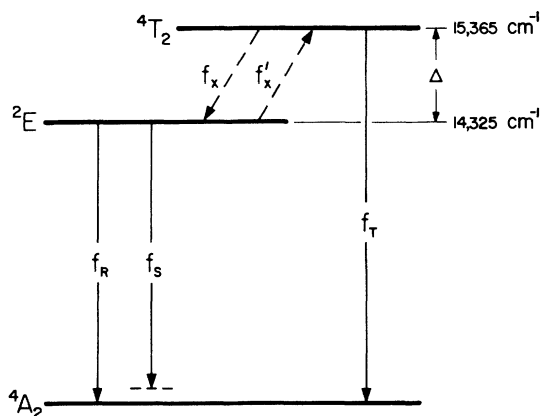


FIG. 9. Simplified energy-level diagram for cubic-site Cr^{3+} ions.

states of the Cr^{3+} ions in cubic sites, since at these temperatures the 4T_2 state acquires a detectable degree of steady-state population under optical pumping.^{13,21} We attribute the broadband luminescence seen in Fig. 7(b) to such 4T_2 luminescence. We separate the R line from the rest of the spectrum by the dotted curve, and the broadband 4T_2 emission from the R line sidebands by the broken curve. This separation into three components, R line, sidebands, and broadband, whose intensities we denote by I_R , I_S , I_T , respectively, was made at a number of different temperatures between 300 and 400 K.

The expected luminescence behavior of the Cr^{3+} ions in cubic sites can be found with the aid of the simplified energy-level diagram of Fig. 9. f_R , f_S , and f_T are the radiative transition probabilities for the R line, for the sidebands of the R line, and for the ${}^4T_2 \rightarrow {}^4A_2$ transition, respectively. We assume that the value of f_R is a constant independent of temperature.²¹ We neglect nonradiative transitions between 2E and the ground state, and between 4T_2 and the ground state. f_x and f'_x are the nonradiative transition probabilities between 4T_2 and 2E as shown in the figure. These are related by $f'_x = f_x e^{-\Delta/kT}$. Since the value of f_x is expected to be much greater than either f_R , f_S , or f_T , the ratio of the populations in the 4T_2 and 2E states is expected to be $3e^{-\Delta/kT}$, where the factor of 3 comes from the greater statistical weight of the 4T_2 state.

f_S should vary with temperature as^{21,22}

$$f_S(T) = f_R \sum_i A_i \coth\left(\frac{\hbar\omega_i}{2kT}\right), \quad (2)$$

where the ω_i 's are the phonon frequencies, and $\sum_i A_i$ gives the intensity ratio of sidebands to R line measured at low temperatures. This ratio

was measured as 4.0 in our sample, which is somewhat smaller than that obtained by Castelli and Forster.⁶ The broken curve in Fig. 10 shows the intensity of the sidebands relative to the R line as predicted by Eq. (2). The full circles give the experimentally measured values of I_S/I_R , and these are seen to fall on the predicted curve. The open circles in Fig. 10 give the experimentally measured values of $(I_S + I_T)/I_R$, from which we can now get I_T/I_R . This ratio should vary as

$$I_T/I_R = 3f_T/f_R e^{-\Delta/kT}, \quad (3)$$

where Δ is the ${}^4T_2 - {}^2E$ separation (about 1040 cm^{-1} at low temperatures). A semilog plot of the measured values of I_T/I_R against I/T is shown in Fig. 11, and it has the predicted straight-line character, with a slope which corresponds to $\Delta = 1100 \text{ cm}^{-1}$ —quite close to the known separation of the 4T_2 and 2E levels. This reinforces our interpretation of the broad emission band which is seen at higher temperatures, and which has the same lifetime as the R line, as being due to ${}^4T_2 \rightarrow {}^4A_2$ luminescence from Cr^{3+} ions in cubic sites. From the data we also obtain a value for f_T/f_R of $\sim 10^3$.

The lifetime τ of the cubic-site luminescence is given by

$$\frac{1}{\tau(T)} = \frac{f_R + f_S(T) + 3f_T e^{-\Delta/kT}}{1 + 3 e^{-\Delta/kT}}, \quad (3)$$

where we assume that f_T is a constant independent

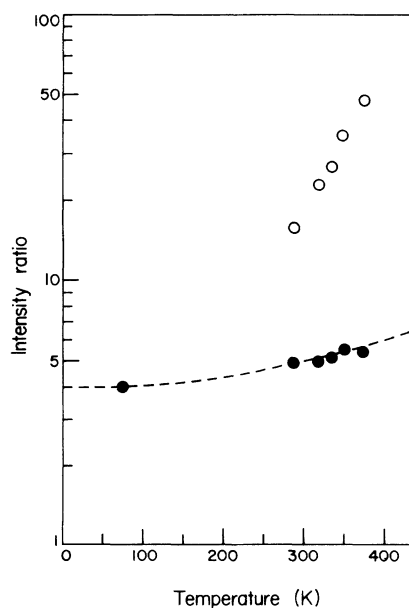


FIG. 10. Full circles give the measured values of I_S/I_R for cubic-site emission as a function of temperature. The broken curve gives the predicted temperature dependence of I_S/I_R . The open circles give the measured values of $(I_S + I_T)/I_R$ as a function of temperature.

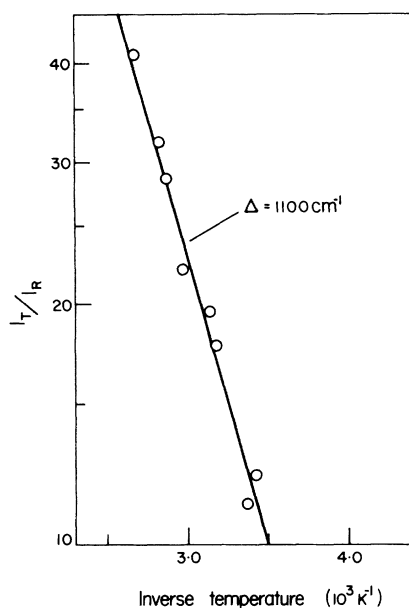


FIG. 11. Semilog plot of I_T/I_R as a function of $1/T$. The data has the predicted $e^{-\Delta/kT}$ dependence where $\Delta = 1100 \text{ cm}^{-1}$.

of temperature. At low temperatures we get

$$1/\tau(0) = f_R + f_S(0) \quad (4)$$

Knowing the value of $\tau(0)$, which is 11.6 msec in our sample, and knowing the ratio of $f_S(0)$ to f_R we find that $f_R = 17.25 \text{ sec}^{-1}$. With this value for f_R we estimate $f_T = 1.7 \times 10^4 \text{ sec}^{-1}$, a typical value for the ${}^4T_2 \rightarrow {}^4A_2$ radiative transition rate.

We are able to explain the temperature dependence of the cubic-site luminescence in a satisfactory way without including nonradiative transitions. Consequently, we believe that such transitions are weak, but because of the crudeness of our data—especially in the separation of sideband and broad band luminescences—we are unable to estimate the contribution of nonradiative transitions to the decay processes.

VIII. CONCLUSION

We have shown that phase-sensitive detection methods afford us a simple means of separating two overlapping luminescence signals from dif-

ferent centers. Using this technique, we have separated the fast-decaying component of the $\text{MgO}:\text{Cr}^{3+}$ luminescence from the remainder of the spectrum. In addition to the broad emission a no-phonon line is found which is normally masked by the stronger emission from the other centers. We show that the centers which are responsible for the fast-decaying luminescence have axes of symmetry along [011]-type directions. This supports the conclusion of Castelli and Forster⁶ that Cr^{3+} ions in rhombic sites are responsible for this luminescence. The main features of the full $\text{MgO}:\text{Cr}^{3+}$ luminescence spectrum would now seem to be understood. Emission from the lowest excited state (2E) of the Cr^{3+} ions in cubic sites gives rise to the R line and its vibrational sidebands. At high temperatures broad emission from the 4T_2 state of these cubic-site ions is also observed. The lines at 6992 and 7038 Å, together with their vibrational sidebands, originate on the 2E level of Cr-vacancy centers, where the vacancy is in a nearest-neighbor Mg^{2+} site along [001]-type directions (tetragonal sites). The lines at 6989 and 7035 Å would seem to originate on the 2E level of Cr-vacancy-Cr centers in a [001]-type orientation. The fast-decaying component, which is observed as a broadband emission stretching from the region of 7000 Å to 1 μm, is due to emission from the lowest excited state (4T_2 in this case) of Cr-vacancy centers, where the vacancy is in the nearest neighbor Mg^{2+} site along [011]-type directions (rhombic sites). Polarization measurements indicate that some weak lines seen in the vicinity of the N lines could originate on Cr^{3+} ions in centers of [001]-type symmetry. These could be due to Cr-vacancy- M centers, where M is an impurity metal cation. Such centers have been found in EPR measurements.^{23,24}

ACKNOWLEDGMENTS

We wish to thank Dr. F. Castelli and Dr. L. S. Forster for communicating their results to us prior to publication. We have benefited from discussions with M. D. Sturge and B. Henderson. One of us (M.O.H.) wishes to thank the Irish Department of Education for a maintenance allowance during the course of this work. This research was supported by the Irish National Science Council.

¹J. E. Wertz and P. Auzins, Phys. Rev. **106**, 484 (1957).

²J. H. E. Griffiths and J. W. Orton, Proc. Phys. Soc. Lond. **73**, 948 (1959).

³B. Henderson and J. E. Wertz, Adv. Phys. **17**, 749 (1968).

⁴A. L. Schawlow, J. Appl. Phys. **33**, 395 (1962).

⁵G. F. Imbusch, A. L. Schawlow, A. D. May, and S.

Sugano, Phys. Rev. **140**, A830 (1965).

⁶F. Castelli and L. S. Forster, Phys. Rev. B **11**, 920 (1975).

⁷Y. Tanabe and S. Sugano, J. Phys. Soc. Jpn. **9**, 766 (1954).

⁸J. P. Larkin, G. F. Imbusch, and F. Dravnieks, Phys. Rev. B **7**, 495 (1973).

⁹A. M. Glass, J. Chem. Phys. **46**, 2080 (1967).

- ¹⁰G. F. Imbusch, Microwave Laboratory Rept. No. 1190, Stanford University, 1964 (unpublished).
- ¹¹G. Peckham, Proc. Phys. Soc. Lond. 90, 657 (1967).
- ¹²J. H. Parker, R. W. Weinert and J. C. Castle, in *Optical Properties of Ions in Crystals*, edited by H. M. Crosswhite and H. W. Moos (Wiley, New York, 1967), p. 251.
- ¹³P. Kisliuk and C. A. Moore, Phys. Rev. 160, 307 (1967).
- ¹⁴H. Engstrom and L. F. Mollenauer, Phys. Rev. B 7, 1616 (1973).
- ¹⁵J. Lambe and W. D. Compton, Phys. Rev. 106, 684 (1957).
- ¹⁶C. Z. van Doorn, Philips Res. Rep. 12, 309 (1957).
- ¹⁷E. J. West and W. D. Compton, Phys. Rev. 108, 576 (1957).
- ¹⁸P. P. Feofilov, Dokl. Akad. Nauk. SSSR 92, 743 (1953).
- ¹⁹W. M. Fairbank, Jr., and G. K. Klauminzer, Phys. Rev. B 7, 500 (1973).
- ²⁰J. Marguglio and Yong Moo Kim, J. Chem. Phys. 62, 1497 (1975).
- ²¹J. P. Hehir, M. O. Henry, J. P. Larkin, and G. F. Imbusch, J. Phys. C 4, 3258 (1974).
- ²²L. S. Forster, in *Transition Metal Chemistry*, edited by R. L. Carlin (Marcel Dekker, New York, 1969), p. 10.
- ²³J. E. Wertz and P. Auzins, J. Phys. Chem. Solids 28, 1557 (1967).
- ²⁴B. Henderson and T. P. P. Hall, Proc. Phys. Soc. Lond. 90, 511 (1967).

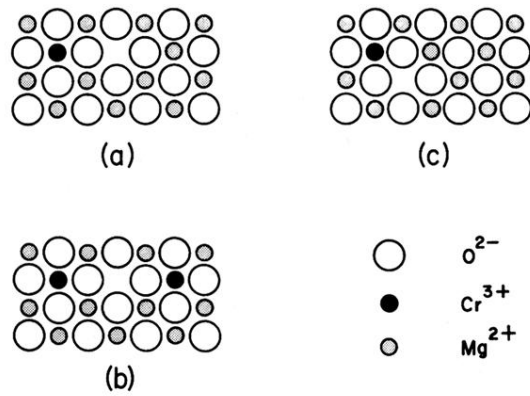


FIG. 2. Representation of the yz plane of MgO showing the environments of Cr^{3+} ions in noncubic sites: (a) tetragonal Cr-vacancy center, [001] symmetry; (b) tetragonal Cr-vacancy-Cr center, [001] symmetry; (c) rhombic Cr-vacancy center, [011] symmetry.